

Adsorption on a polar oxide surface: O₂, C₂H₄ and Na on Cr₂O₃(0001)/Cr(110)

Bernd Dillmann, Friedmann Rohr, Oliver Seiferth, Gabor Klivenyi,
Michael Bender, Klemens Homann, Ivan N. Yakovkin, Daniela Ehrlich,
Marcus Bäumer, Helmut Kühlenbeck and Hans-Joachim Freund*

Fritz-Haber-Institut der Max-Planck-Gesellschaft, Faradayweg 4-6, 14195 Berlin,
Germany
and Lehrstuhl für Physikalische Chemie I, Ruhr-Universität Bochum, 44780 Bochum,
Germany

A polar Cr₂O₃(0001) surface is prepared as an epitaxial film on a Cr(110) substrate. The film is thick enough to represent the bulk surface. Applying a variety of surface sensitive techniques [thermal desorption spectroscopy (TDS), reflection absorption infrared spectroscopy (RAIRS), electron energy loss spectroscopy (EELS) and photoelectron spectroscopy (PES)] we have studied adsorption of molecular oxygen, ethene and sodium.

Introduction

The physics and chemistry of oxide surfaces have received increasing attention recently.^{1–38} There are several books and review articles that cover various aspects of the field.^{1–9} As a specific issue, the comparison of non-polar and polar surfaces of insulating oxides is interesting from a chemical point-of-view, because of the higher energy content of polar surfaces, which can be used to drive restructuring processes.⁸ Although it appears to be very difficult to prepare polar surfaces *via* cleavage of bulk single crystals, preparation as thin films is straightforward. It has been demonstrated for MgO(111)²⁶ and NiO(111)³⁹ that surface reconstruction^{22,23} plays a prominent role for the clean surface. If, however, the surface is hydroxy-terminated for NiO(111)³⁹ we find a $p(1 \times 1)$ LEED pattern, characteristic of the ideal hexagonal surface. The reconstruction of the clean, polar rocksalt surfaces involves rather massive mass transport indicating that the mobility of the surface constituents can be large. In particular, the so-called octopolar reconstruction^{22,23} extends throughout the first two layers of the (111) surface in order to compensate the diverging surface potential. For corundum surfaces the reduction of charge in the surface layer has been suggested to occur *via* removal of half of the number of surface ions, thus formally only taking place in the topmost layer.^{1,40–45} However, we know from a recent LEED I/V-study⁴⁵ of a Cr₂O₃(0001) surface that very pronounced relaxations occur between several layers near the surface, such relaxations are in line with theoretical predictions for (0001) surfaces of corundum-type oxides.^{46,47} As a prototype corundum surface we have investigated, in this study, adsorption and reaction of small molecules such as O₂ and ethene on a Cr₂O₃(0001) surface, as well as adsorption of Na (to include a metallic adsorbate) by applying a variety of experimental techniques, such as TDS, EELS, PES, LEED and RAIRS.

Experimental

A chromium oxide film with (0001) orientation was grown on a Cr(110) surface *via* oxidation and thermal treatment cycles.^{40–45} The order of the film was checked *via*

LEED, and the stoichiometry *via* X-ray photoelectron spectroscopy (XPS). Ion scattering spectroscopy (ISS) was used to determine that the average surface coverage of chromium ions was 50% of the bulk terminated surface.⁴³ Recipes for oxide film preparation have been published before.^{40–45} The sample is attached to a holder that can be cooled to liquid-nitrogen temperature, and heated up to 1000 K (high enough to desorb thermally the oxide films). Experiments were performed within several ultrahigh vacuum (UHV) systems. One system contained a combined angle resolved photoemission (ARUPS) set-up and an electron monochromator for EELS measurements. [An equivalent ARUPS set-up is available at the Berliner Elektronenspeicherring (BESSY).] The preparation chamber contained facilities for TDS measurements. The second system had set-ups for high-resolution EELS and RAIRS. A third system was dedicated to XPS studies. The gases were used as purchased, and they were of at least 99.9% purity. Na was dispensed from a commercial SAES-getter, which was mounted within a small tantalum box having a small opening. Evaporation onto the surface was started by removing a shutter from the Na dispenser opening.

The sodium coverage was calibrated by cross-reference to a previous experiment in which magnesium had been grown epitaxially on a clean Cr(110) surface⁴⁸ in the same chamber. The XPS intensities of the corresponding Mg and Na 1s photoemission lines were measured in identical sample positions in both cases. An Mg 1s XPS intensity of 1.8 ± 0.2 corresponded to an Mg atom density of $7.5 \times 10^{14} \text{ cm}^{-2}$ in a hexagonal Mg(0001) monolayer. The cross-referencing accounts for the different ionization cross-sections of the Na 1s ($\sigma = 0.1781$) and Mg 1s ($\sigma = 0.1524$) lines taken with Al-K α and Mg-K α radiation, respectively. The calculated ionization cross-sections are taken from ref. 49. The different photon fluxes of both X-ray tubes are corrected by normalizing the line intensity to the background intensity. By rescaling the Na 1s line intensity, a value of 1.8 corresponds to a sodium atom density of $6.4 \times 10^{14} \text{ cm}^{-2}$. We define a monolayer as one sodium atom per (1 \times 1) unit mesh, which has an area of $21.65 \times 10^{-16} \text{ cm}^2$ on the clean Cr₂O₃(0001) surface. The corresponding sodium atom density is then $4.6 \times 10^{14} \text{ cm}^{-2}$. The error, is estimated on the basis of the experimental results to be 10%.

Results and Discussion

We present and discuss the results of the three different adsorbate systems separately but it will become obvious that the results are interdependent.

Oxygen adsorption

As was shown in an earlier preliminary study on oxygen adsorption on clean Cr₂O₃(0001) the molecule adsorbs at 90 K surface temperature and can be partly desorbed near room temperature.⁴⁰ It was suggested, but not proven, that below room temperature O₂ is associatively adsorbed and that it partly dissociates at or above room temperature. HREEL spectra showed an additional feature near 1000 cm^{-1} , present after O₂ adsorption, that increased in intensity and shifted to higher frequency upon heating above 300 K. As O₂ is a homonuclear diatomic it does not exhibit an IR spectrum in the gas phase. However, from Raman studies the frequency is known to be 1554.7 cm^{-1} .⁵⁰ The decrease in the stretching frequency was interpreted as being compatible with the formation of O₂⁻.^{40,51} more or less perpendicularly oriented with respect to the surface. A comparison with peroxy- and superoxy-species in complexes and on metal surfaces substantiated the argument.^{52,53} It was also discussed in the earlier paper that O₂ dissociation can lead to the formation of chromyl species (Cr=O) on the surface. Evidence for this was provided by the vibrational frequency observed: CrO₂Cl₂ exhibits Cr=O stretching⁵⁴ frequencies very close to those observed for the O₂

adsorbate system. It is conceivable that O_2 dissociation leads to the formation of chromyl species with either one $Cr=O$ double bond or two geminal $Cr=O$ bonds, as in the $Cr_2O_2Cl_2$ compound. Owing to the presence of two $Cr=O$ double bonds in CrO_2Cl_2 , two modes, one antisymmetric (out-of-phase) and one symmetric (in-phase), are observed in the compound spectra. The limited resolution of the HREELS experiment⁴⁰ did not allow separation of the two modes, which differ by 10 cm^{-1} in frequency. In general, the earlier studies did not clearly identify oxygen dissociation, and, in particular, a detailed mechanistic discussion on how dissociation could take place was not possible on the basis of the earlier data. However, this is a very interesting problem because it provides insight into whether and how oxygen from the gas phase could be incorporated into the oxide lattice of the oxide film and thus into film growth.⁵⁵ The fact that this can strongly influence the defect structure of the film and therefore the chemical properties of the surface makes the problem even more interesting.

Fig. 1 shows the TD spectra of O_2 on $Cr_2O_3(0001)$.⁵⁶ Various coverages are compared by observing the partial pressures of m/z 16 and 32. We find a rather structured spectrum at desorption temperatures of between 110 and 320 K. Obviously, an interpretation of the features between 110 and 220 K is complex, and contains states in dynamical equilibrium with each other. The TD spectra are all dominated by a feature with a maximum temperature between 290 and 330 K. The saturation coverage of oxygen is 5 L and the TD spectra do not change after higher exposures, clearly showing that there is no multilayer adsorption of oxygen at 90 K. All the peaks are due to molecular desorption out of molecularly adsorbed states. In other words, there is no recombinative desorption in any of these cases. This is clearly demonstrated by the TD spectra in Fig. 2. Here the surface was dosed with a mixture of equal amounts of $^{16}O_2$ and $^{18}O_2$. On the right hand side of the figure the two, simultaneously recorded, mass spectra at m/z 32 and 36 are shown. A pressure calibration shows that the intensity is well within the

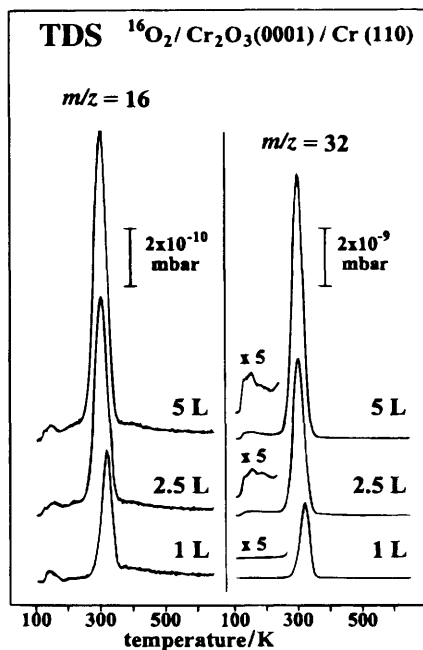


Fig. 1 TD spectra after adsorption of different amounts of $^{16}O_2$ on $Cr_2O_3(0001)/Cr(110)$ at 90 K. The heating rate was 4 K s^{-1} . The intensity of $m/z = 16$ (left side) and $m/z = 32$ (right side) is shown.

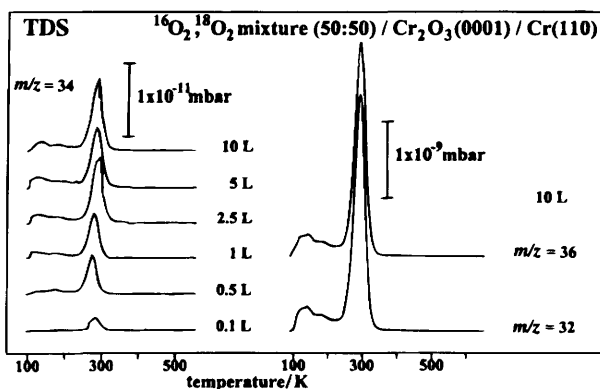


Fig. 2 TD spectra after adsorption of a 50 : 50 mixture of $^{16}\text{O}_2$ and $^{18}\text{O}_2$ on $\text{Cr}_2\text{O}_3(0001)/\text{Cr}(110)$ at 90 K. The heating rate was 4 K s^{-1} . On the left hand side the intensity of $m/z = 34$ after different dosages of this mixture is shown. On the right hand side the intensity of $m/z = 32$ and $m/z = 36$ after a dosage of 10 L of this mixture is shown.

range of 10^{-9} mbar for both masses. If O_2 dissociation played an important role in the interpretation of the spectra one would expect TD spectra recorded for the mixed mass $^{16,18}\text{O}_2$, *i.e.*, m/z 34, to have considerable intensity. The corresponding spectra are shown for various dosages on the left hand side of Fig. 2. Clearly there is a signal but its intensity is more than two orders of magnitude lower than in the spectra on the right hand side. It is of the correct order of magnitude to be explained by contaminants in the isotopically labelled compound. This means that exchange, *i.e.*, through dissociation, only plays a very minor role for this feature in the TD spectrum.

However, dissociation does occur on the surface, as will become evident from the following discussion of the IR spectra. Fig. 3 shows a set of IR spectra between 90 and 780 K after dosing 6 L at 90 K. On the left hand side, the spectra are obtained after dosing $^{16}\text{O}_2$, on the right hand side after dosing $^{18}\text{O}_2$. At the lowest temperature a broad peak centred around 990 cm^{-1} ($^{16}\text{O}_2$) and 930 cm^{-1} ($^{18}\text{O}_2$), respectively, shows

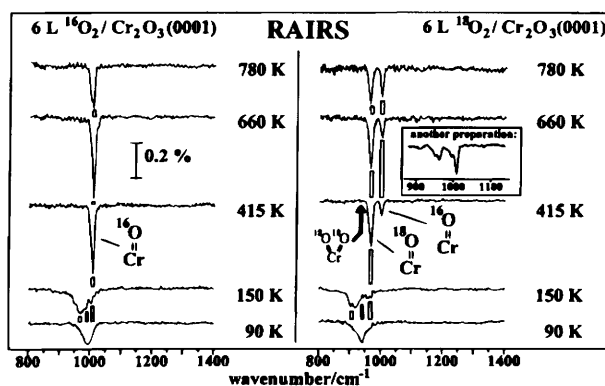


Fig. 3 RAIR spectra after adsorption of a saturation coverage of $^{16}\text{O}_2$ (left side) and $^{18}\text{O}_2$ (right side) on $\text{Cr}_2\text{O}_3(0001)/\text{Cr}(110)$ at 90 K. At the bottom the spectra are recorded after adsorption at 90 K. The other spectra are taken after heating to different temperatures. Shown are absorption signals of molecular and atomic oxygen species. The inset on the right hand side shows the absorption signals of the chromyl bands (atomic oxygen) from a slightly differently prepared oxide film.

up. Whereas there is only slight intensity at 965 cm^{-1} ($^{16}\text{O}_2$) and 905 cm^{-1} ($^{18}\text{O}_2$) initially this intensity increases to form another broad band as the surface temperature rises to 150 K. At this temperature, or a little below, another spectral feature, (which eventually develops into a rather sharp peak) starts to show up at 1005 cm^{-1} (^{16}O) and at 960 cm^{-1} (^{18}O). For the $^{16}\text{O}_2$ dosage a single relatively sharp feature grows until the surface reaches a temperature of 660 K, then it starts to decrease again. For the $^{18}\text{O}_2$ dosage two sharp features at 960 cm^{-1} and 1005 cm^{-1} are observed. The peak at 1005 cm^{-1} gains in intensity as the temperature increases. Depending somewhat on the preparation conditions of the Cr_2O_3 film the sharp feature can be split by approximately 10 cm^{-1} , as shown in the inset.⁵¹ Also all the measured frequencies were compatible with the previously published HREELS data.⁴⁰ We note at this point that the oxide film was grown using $^{16}\text{O}_2$, *i.e.*, before the adsorption experiments were carried out. If the oxide film is grown using $^{18}\text{O}_2$ the IR spectra after adsorption of oxygen, $^{16}\text{O}_2$ or $^{18}\text{O}_2$, respectively, did not show any difference in comparison to the spectra from the $\text{Cr}_2^{16}\text{O}_3$ film.

On the basis of the TD spectra it is quite obvious that the broad features observed below 150–220 K are due to molecularly adsorbed O_2 . In fact, it is probably the features with maximal intensities at 965 cm^{-1} ($^{16}\text{O}_2$) and 905 cm^{-1} ($^{18}\text{O}_2$), which become more prominent in the RAIR spectra after heating to 150 K, that lead to the strong desorption feature at 300 K. The higher frequency peak at 990 cm^{-1} ($^{16}\text{O}_2$) and 930 cm^{-1} ($^{18}\text{O}_2$) could be associated with the O_2 molecules desorbed at lower temperatures, which is indicative of a smaller interaction with the substrate. The shift could also be due to the change in intermolecular interaction. The adsorbed molecular species show a stretching frequency rather different from the gas phase value (1554.7 cm^{-1}).⁵⁰ The frequency shifts with respect to the gas phase, are similar to those observed for peroxo- or superoxo-compounds,^{53,57} which nominally contain an O_2^{2-} or an O_2^- moiety.

While the Cr 2p XPS data indicate a charge transfer from the surface to the O_2 moiety^{40,58} this charge transfer is rather small, as revealed by the EELS data⁵¹ shown in Fig. 4. The O_2 physisorbed onto a thin Al_2O_3 film (upper trace) is excited with electrons⁵⁹ and the loss features in the range 0.5–2.5 eV are considered. The two sharp excitations are known from the gas phase to be due to the $^1\Delta_g$ and the $^1\Sigma_g^+$ of O_2 .⁵⁰ The survival of the gas phase spin structure proves the physisorbed nature of the adsorbed molecule. In the lower trace a clean $\text{Cr}_2\text{O}_3(0001)$ surface is excited exhibiting the d–d excitations of the Cr^{3+} ions in the surface (as has been discussed in detail before⁴²). The trace in the middle shows this loss range after a saturation dosage of O_2 at 90 K.⁵¹ The number of features and their relative intensities do not depend on the O_2 dose. Obviously the oxygen-induced excitations are in the same energy range as those of the physisorbed O_2 and of the Cr^{3+} surface excitations. As compared with the physisorbed case the excitations are broader indicating a stronger interaction with the surface and shorter lifetimes of the excited states. The spectra can be interpreted qualitatively on the basis of orbital schemes also shown in an inset in Fig. 4. For gas phase, as well as physisorbed oxygen, the O–O bonding π -orbitals (π_u) are fully occupied and degenerate, the O–O antibonding π -orbitals (π_g) are half occupied and also degenerate. Within this orbital scheme group theory yields six possible states, namely a triplet and a singlet manifold each with three spatial symmetries ($\Sigma_{u,g}^+$, $\Sigma_{u,g}^-$, $\Delta_{u,g}$). The ground state is the $^3\Sigma_g^-$ state and the lowest lying excited states are $^1\Delta_g$ and $^1\Sigma_g^+$.⁵⁰ If the molecule is coupled to a surface, perhaps *via* a chromium ion, the symmetry is broken and the orbital degeneracy is removed. Depending on the strength of the interaction and/or the number of electrons transferred into the orbital scheme, the electronic excitations are shifted and the degenerate excitations split. Although this has to be studied theoretically in detail in the future, we think that a strong coupling, implying extensive mixing of O_2 and substrate wavefunctions (which could lead to a full electron transfer) would shift the O_2 excitations more than was found experimentally.

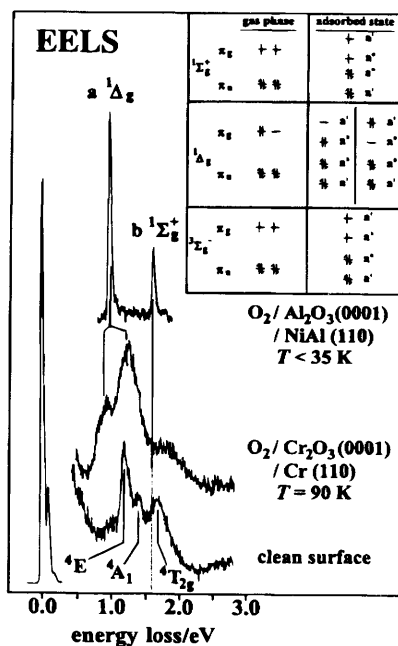


Fig. 4 EEL spectra after adsorption of oxygen on $\text{Al}_2\text{O}_3(0001)/\text{NiAl}(110)$ at 35 K and on $\text{Cr}_2\text{O}_3(0001)/\text{Cr}(110)$ at 90 K. At the bottom the EEL spectrum from the clean Cr_2O_3 surface is shown. The lowest lying electronic excitations of the adsorbed oxygen molecule are shown. The inset illustrates the splitting of the oxygen-induced peaks because of a more strongly adsorbed oxygen molecule on $\text{Cr}_2\text{O}_3(0001)$. The electron configurations given in the inset form linear combinations to represent the excited states of the adsorbed molecule.

The data are compatible with an O_2 molecule moderately (covalently) interacting with the substrate and inducing only a small charge-transfer. This would also be consistent with an oxygen molecule, that leads to an O—O vibrational absorption in the region around 1000 cm^{-1} . It is important to note, of course, that upon heating above room temperature, the transitions in the EEL spectrum disappear, however, the Cr^{3+} surface excitations do not reappear, indicating that there is still surface oxygen present. Effectively, the oxidation state of the surface chromium ions has increased after dissociation. This surface oxygen gives rise to the sharp feature in the RAIR spectra. The observed frequency is typical for $\text{Cr}=\text{O}$ bonds as found in chromyl compounds. The isotope shift for $\text{Cr}=\text{O}$ is smaller as compared with the isotope shift for $^{18}\text{O}_2/^{16}\text{O}_2$ adsorption. The fact that for certain conditions the $\text{Cr}-\text{O}$ vibrational mode is split (see Fig. 3), is compatible with two different mono-oxo ($\text{Cr}=\text{O}$) species on the surface, whose relative concentrations would depend on the preparation conditions. However, it would also be consistent with a CrO_2 species, as in CrO_2Cl_2 , with two $\text{Cr}=\text{O}$ bonds at one chromium ion. In fact, the splitting observed is very close to the difference between the in-phase and out-of-phase stretching normal modes of CrO_2Cl_2 as mentioned above. The present isotopic labelling data reveal instead the existence of single $\text{Cr}=\text{O}$ bonds. Consider again Fig. 3 and let us assume for the moment that the vibration at 1005 cm^{-1} is due to $^{16}\text{O}-\text{Cr}-^{16}\text{O}$, as in $\text{Cr}_2\text{O}_2\text{Cl}_2$. If we expose a $\text{Cr}_2^{16}\text{O}_3(0001)$ surface to $^{18}\text{O}_2$ we would have to expect the formation of $^{18}\text{O}-\text{Cr}-^{18}\text{O}$, $^{18}\text{O}-\text{Cr}-^{16}\text{O}$ and $^{16}\text{O}-\text{Cr}-^{16}\text{O}$ for the adsorbed dissociated oxygen, because it might exchange with the lattice oxygen. Indeed, as the temperature increases the right hand side of Fig. 3 indicates the formation of a second band, but a third band has never been observed under these conditions. The frequency of the first band (1005 cm^{-1}) occurring after adsorption

of $^{18}\text{O}_2$ is identical to the one found for $^{16}\text{O}_2$ exposure. Since we have assumed within the present argument that this band is due to $^{16}\text{O}-\text{Cr}-^{16}\text{O}$ with two $\text{Cr}=\text{O}$ bonds, the observation of only two bands would indicate that there is no $^{18}\text{O}-\text{Cr}-^{18}\text{O}$ species, which is unreasonable from a statistical point-of-view. The position of the expected $^{18}\text{O}-\text{Cr}-^{18}\text{O}$ mode is shown in Fig. 3. Therefore, we come to the conclusion that dissociation of O_2 leads to the formation of chromyl species with single $\text{Cr}=\text{O}$ bonds on the surface similar to the situation found for polycrystalline samples.⁶⁰

Although the chromyl oxygen might exchange with the lattice oxygen, there is evidence that not all of the ^{16}O chromyl oxygens stem from the oxide lattice. The evidence for this is shown in Fig. 5. On the left hand side the surface signal is shown after cleaning the $\text{Cr}_2^{18}\text{O}_3(0001)$ surface by a temperature flash (830 K). Concurrently, the sample is heated in steps to the given temperature for fixed time. Obviously, the heat treatments led to the formation of chromyl groups even at the formerly clean surface. This process continues until saturation is reached. Even if the surface is partially covered by chromyl groups, isotopically labelled as $\text{Cr}-^{18}\text{O}$, the surface saturates with ^{16}O chromyl groups as indicated by the increase in intensity in the $\text{Cr}-^{16}\text{O}$ vibrational mode. This is shown on the right hand side of Fig. 5. Such processes even occur on an oxide film prepared with $^{18}\text{O}_2$, as shown in Fig. 5, leading to the conclusion that the oxygen stems from the underlying chromium crystal or from background contamination.⁵⁵ The oxygen, which is well known as a major impurity in single crystal chromium,⁶¹ seems to segregate through the oxide film to the surface, then forms the ^{16}O chromyl species. The atomically adsorbed oxygen desorbs at about 830 K, this is becoming clear from Fig. 5. The surface coverage with chromyl groups is relevant for the chemical activity of the surface. While the chromyl covered surface is rather inert, removal of the chromyl oxygen considerably increases the chemical activity of the surface.⁶²

This becomes relevant if we try to adsorb other molecular species, such as ethene, onto the $\text{Cr}_2\text{O}_3(0001)$ surface and then study the influence of pre-adsorbed oxygen on reactivity.⁶²

Ethene adsorption

Before we ask the question of how oxygen influences ethene adsorption, the adsorption of ethene onto the clean $\text{Cr}_2\text{O}_3(0001)$ surface will be discussed. Fig. 6 shows the C_2H_4 TD spectra of the clean $\text{Cr}_2\text{O}_3(0001)$ surface as a function of initial dosage at 90 K.⁶²

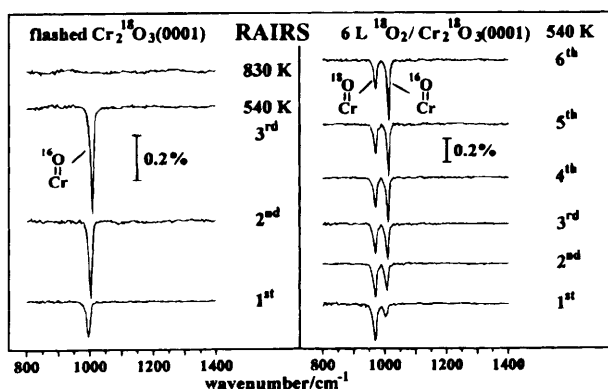


Fig. 5 RAIR spectra taken from clean $\text{Cr}_2^{18}\text{O}_3(0001)/\text{Cr}(110)$ at 90 K (right side) after heating the sample for several times to 540 K. At the top a spectrum is shown after heating to 830 K. On the left hand side RAIR spectra are shown taken after adsorption of a saturation coverage (6 L) of $^{18}\text{O}_2$ on $\text{Cr}_2\text{O}_3(0001)/\text{Cr}(110)$ at 90 K and subsequent heating to 540 K several times.

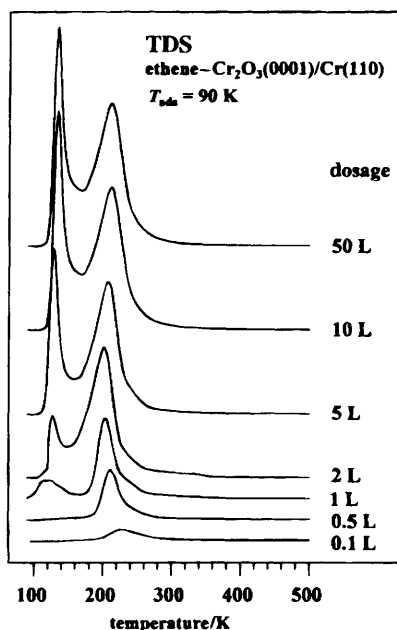


Fig. 6 TD spectra of C₂H₄/Cr₂O₃(0001)/Cr(110) as a function of initial ethene coverage

There are two adsorbate states that can be identified on the basis of the spectra. One, with a desorption temperature maximum shifting from 220 K at lower dosage to 210 K at higher dosage, and a second one with a desorption temperature maximum shifting from 120 K to 130 K as the dosage increases. At very low exposures there is a small quantity of molecules desorbed at 240 K.

The RAIR spectra shown in Fig. 7 allows a more detailed characterization of the molecule-substrate interaction.⁶² In Fig. 7(a) the spectra are plotted as a function of ethene dosage. The frequency regions chosen cover the C-H out-of-plane wagging mode γ_{ω} and the symmetric C-H stretch mode ν_{sym} of the ethene molecule. Note, that at the temperature range chosen for C₂H₄ IR studies, the formation of chromyl groups (Cr=O) on the surface can be excluded. At lower dosage two wagging modes are observed shifted by 6 cm⁻¹ with respect to each other. The intensity of the C-H stretch is below the signal-to-noise ratio of the background. As the C₂H₄ dose increases above 1 L we do find the occurrence of a C-H stretch intensity and in parallel an additional shoulder in the range of the C-H wagging mode indicative of a second species with different vibrational properties. With increasing coverage the linewidth of the vibrational modes increases as well, which is in line with expectations.

Let us first consider the absence of the symmetric C-H stretch at low coverage. Comparing the coverage dependence of the RAIR spectra with the TD spectra we realise that at 1 L, desorption from the more weakly adsorbed state is observed. This coincides, more or less, with the occurrence of the symmetric C-H stretch while the weakly bound state shows a C-H stretch mode. In other words, the more strongly bound state is characterized by the absence of a symmetric C-H stretch. This is a very strong indication of a geometric orientation effect for the more strongly bound molecules.⁶³

Briefly, the symmetric C-H stretching vibration produces a dynamic dipole, which is oriented within the molecular plane. If the molecule itself is oriented parallel to the surface and the relative permittivity of the substrate material is such that a dynamic image dipole is induced, the superposition of the two dynamic dipoles leads to a quen-

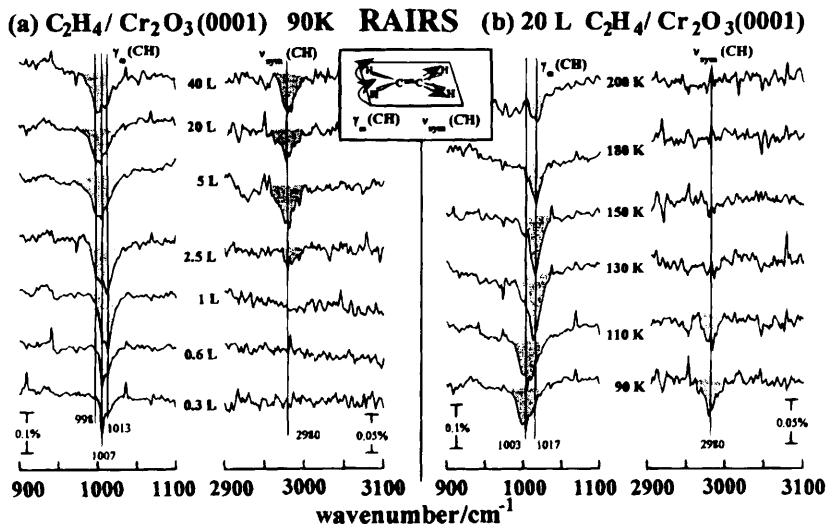


Fig. 7 RAIRS spectra of adsorption of C_2H_4 on $\text{Cr}_2\text{O}_3(0001)/\text{Cr}(110)$. (a) As a function of dosage; and (b) as a function of temperature after dosing 20 L at 90 K.

ching of the IR activity. If the molecular plane and the surface were perpendicular to each other, or include an angle between them, the C—H stretching intensity would not vanish. On the other hand, the C—H wagging mode is not oriented within the molecular plane. Therefore, even if the molecular plane is oriented parallel to the surface there is a component of the dynamic dipole oriented perpendicularly to the surface. Consequently, the dynamic image dipole enhances the effective dynamic dipole and thus the IR band may be observed even at low coverage, as seen in experiment (Fig. 7).

The fact that there are two components of the wagging mode cannot be fully interpreted at present. It could be due to intermolecular coupling, or to inequivalent molecules at steps and terrace sites. The latter interpretation would be consistent with the shift of the desorption maximum from 220 to 210 K in TDS and the relative increase of the RAIRS component at 1013 cm^{-1} for increasing coverage.

Considering the experimental observation for the wagging and the stretching mode together, both findings are consistent with ethene molecules oriented parallel to the $\text{Cr}_2\text{O}_3(0001)$ surface in the more strongly bound state. The desorption temperature of this state points towards a weakly chemisorbed state. XPS measurements published previously reveal a small charge transfer from the ethene molecule to the surface.⁶² The state with a desorption temperature near 130 K would then be termed a physisorbed state. In this state there is no indication from the RAIRS spectra for a preferential adsorption geometry. Both modes are observed above 1 L dosage. Fig. 7(b) confirms the above discussion and shows that the adsorption is fully reversible. In Fig. 7(b) the surface is saturated with ethene at 90 K and is consequently heated to 200 K. At a surface temperature of 130 K the C—H stretch disappears and the C—H wagging mode shifts appropriately.

At this point we come back to the influence that oxygen pre-adsorption might have on ethene adsorption. Fig. 8 compares the TD spectra of ethene adsorption on a clean $\text{Cr}_2\text{O}_3(0001)$ surface with that on an oxygen predosed surface. In general we find that ethene adsorption is partly blocked by oxygen pre-adsorption thus reducing the amount of ethene on the surface.⁶² However, a detailed investigation reveals that the interdependencies are rather complex. If oxygen and ethene are both adsorbed at low temperatures, the molecular adsorption states of O_2 as shown in TDS have counterparts in

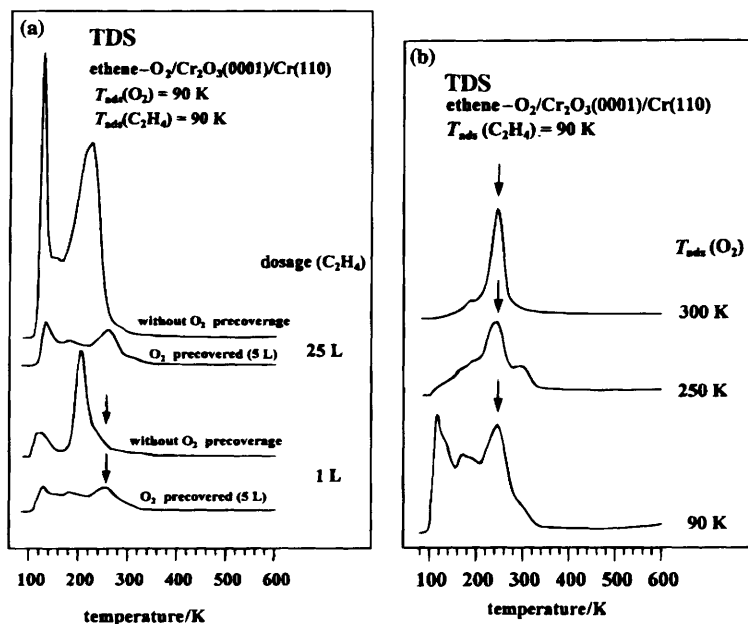


Fig. 8 TD spectra of ethene. (a) On clean and oxygen-predosed $\text{Cr}_2\text{O}_3(0001)$ surface; and (b) on the oxygen-predosed $\text{Cr}_2\text{O}_3(0001)$ surface as a function of oxygen adsorption temperature.

the ethene TD spectra indicating that these molecules might partly exchange. In passing we note that the formation of CO (m/z 28) cannot be fully excluded. One adsorption state of C_2H_4 , however, seems to be strongly influenced by the presence of oxygen. As shown in Fig. 8 the high-temperature desorption peak of weakly chemisorbed ethene appears at 230–240 K (arrows in Fig. 8), a peak that was also found when only small amounts of C_2H_4 were dosed onto the clean surface (Fig. 6, lowest trace). In Fig. 8 we show TD spectra where the surface has been predosed with oxygen at low temperature, then heated to room temperature and consecutively dosed with small amounts of C_2H_4 at different surface temperatures. We find C_2H_4 desorption at 240 K (arrows).

We interpret these results as follows. On heating the oxygen precovered surface to 300 K, the terrace chromium ions react to form chromyl units. Only the chromium ions at steps or sites, which are coordinated, such that the covalent chromyl bonds cannot be formed, can still accommodate an ethene molecule *via* a weak chemisorptive bond, when ethene is dosed. These sites then give rise to the desorption maximum at 240 K. We have checked in this case that the desorbed molecule is not CO by recording the signals at m/z 28 and m/z 27 in parallel. From these observations it is clear that the oxygen concentration at the surface has a strong influence on the reactivity of the system. The reported polymerization of C_2H_4 ^{64,65} on the $\text{Cr}_2\text{O}_3(0001)$ surface at a pressure of 1 bar is,⁶² for example, considerably influenced by oxygen pre-adsorption. We found that oxygen pre-adsorption strongly attenuates the polymerization activity.⁶²

Sodium adsorption

Obviously, ethene induces a small charge transfer towards the surface *via* a weak π -donor bond. For other adsorbate systems, such as alkali metals, we can expect a much more pronounced charge transfer towards the surface, which in turn can strongly influence molecular adsorption of other species.⁶⁶ We know from a study of Na on NiO(111)

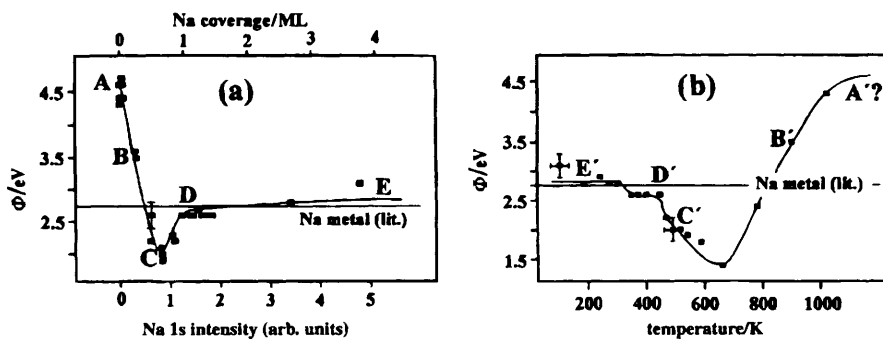


Fig. 9 Workfunction ($\Delta\Phi$) as a function of sodium coverage in: (a) a sodium deposition experiment on $\text{Cr}_2\text{O}_3(0001)/\text{Cr}(110)$ at 90 K; and (b) a heating experiment on multilayers of sodium on $\text{Cr}_2\text{O}_3(0001)/\text{Cr}(110)$. The calculated sodium coverage is given in the top abscissa in (a).

that charge transfer can proceed as far as the formation of metal from the oxide.⁶⁷ It will be seen in the following that for $\text{Cr}_2\text{O}_3(0001)$ reduction to Cr metal does not occur, however, a pronounced charge transfer can be observed.

In a previous study, the attenuation of the Cr_2O_3 Fuchs-Kliewer phonon modes by the deposition of metallic sodium indicated the formation of sodium layers (*via* a rather abrupt decrease) as a function of sodium dosage.⁴¹ Fig. 9(a) shows the workfunction change of the oxide surface at 90 K as a function of sodium coverage. Starting at the workfunction value of the clean $\text{Cr}_2\text{O}_3(0001)$ surface (4.6 eV) (denoted as point A), the workfunction steeply decreases linearly through point B towards a minimum (point C), which is located at a coverage of 0.7 ML, *i.e.*, in the submonolayer regime.

From the slope of the curve in the submonolayer regime the dipole moment of an isolated adsorbed sodium atom can be calculated as usual⁶⁸ to be 2.6 D.† This is in line with theoretical as well as experimental results for alkali atom adsorption on metal surfaces.⁶⁹ Close to monolayer coverage (point D) the workfunction increases again towards the value of sodium metal (point E).⁷⁰ In this latter respect the behaviour of the $\text{Cr}_2\text{O}_3(0001)$ surface is profoundly different from the behaviour of the $\text{NiO}(111)$ surface upon exposure to sodium.⁶⁷ While for $\text{NiO}(111)$ the rather slow increase after passing through the minimum is an indication for the irreversibly occurring chemical reaction, *i.e.*, reduction to nickel metal, on the oxide surface,⁶⁷ the situation for chromium oxide is indicative of a reversible, layered-growth mode involving charge redistribution between adsorbate and surface.

This statement is corroborated by the inverse experiment in which a Cr_2O_3 surface is covered with a thick sodium layer, and is then heated in order to remove the sodium layer. Fig. 9(b) shows the workfunction changes observed in this case. Clearly, the workfunction follows a similar curve, including the characteristic values (E' through B'), reversed with respect to Fig. 9(a). The curves cannot exactly match because the removal rate *via* temperature-programmed desorption is generally different from the deposition rate at a given temperature (here 90 K). Again, the behaviour is very different from $\text{Na}/\text{NiO}(111)$ where heating of a thick layer leads to workfunction changes and extreme values completely at variance with the deposition experiment.⁶⁷

We have followed the electronic changes in the sodium adsorbate and in the oxide substrate as a function of sodium coverage and substrate temperature with various electron spectroscopies, including photoemission of the Na 2p and Cr 2p_{3/2} levels, Auger spectroscopy of the Na L₂₃L₂₃ line, as well as EELS of the surface valence excitations.

† D = 1 D(debye) $\approx 3.33564 \times 10^{-30}$ C m.

We will refer these data to the workfunction curves in Fig. 9(a) and 9(b) by using the labels A–E in the deposition experiments, and A'–E' in the desorption experiments, respectively.

The chemical state of sodium can be investigated purely on the basis of Na 2p photoemission data recorded with the use of synchrotron radiation at the BESSY I storage ring in Berlin. Fig. 10 show a data set recorded *via* a heating experiment. At high sodium coverage a typical spectrum of a metallic layer⁷¹ is observed in the temperature range between 90 and 400 K. As soon as the monolayer regime (D') is reached the spectral function indicates the loss of metallic character *via* the disappearance of the plasmon losses, which is followed by a shift and broadening of the main signal initially located at 30.8 eV. At 420 K we observe two distinct features at 31.5 eV and 33.2 eV binding energy evolving on the timescale of the experiment, *i.e.*, in a few minutes. The former has a binding energy typical of an ionic sodium species. Na 2p binding energies are reported for sodium oxide (31.1 eV)⁷¹ as well as for the sodium halides, NaF (29.8 eV) through NaI (31.1 eV),⁷² in line with this assignment.

The second signal, however, occurs at an abnormally high binding energy as compared with the above mentioned literature values for both metallic and ionic sodium species. In the following discussion we will argue that this might be because of the presence of neutral, isolated sodium atoms on an otherwise clean chromium oxide surface.

The binding energy can be reconciled as the binding energy of sodium atoms in the gas phase corrected by the local workfunction of the substrate, as the atom is brought to the surface. With the binding energy of free sodium atoms being 38.45 eV and 38.03 eV for the ¹P and the ³P final states, respectively,⁷³ we calculate the value for sodium atoms on a clean chromium oxide surface with a workfunction of 4.6 eV to be 33.85 eV and 33.46 eV, respectively, referenced to the Fermi level. The experimental value is found to be 33.2 eV.

According to the latter we emphasize that the signal at 31.5 eV vanishes step-by-step up to a temperature of 540 K. We ascribe this to a penetration of the ionic species into the substrate lattice. Mixed oxide compounds of chromium oxide and alkali oxides are

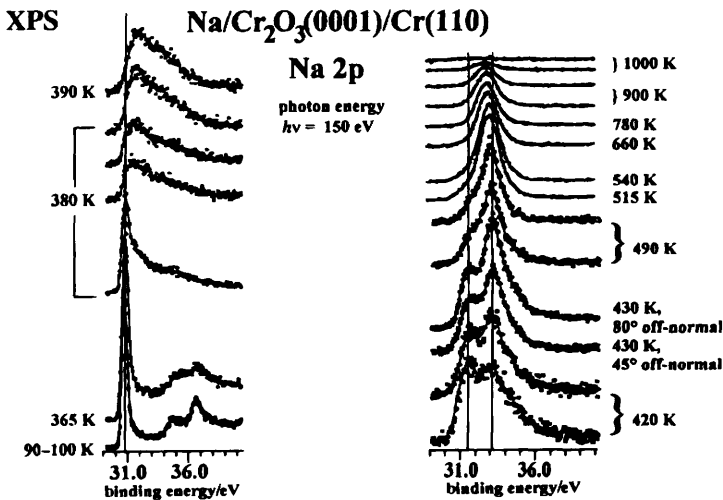


Fig. 10 Na 2p XP spectra of a multilayer sodium deposit on $\text{Cr}_2\text{O}_3(0001)/\text{Cr}(110)$ as a function of temperature. The temperature was kept constant during spectra recording. The braces indicate single scan spectra taken isothermally after each other.

known to have a hexagonal-layered structure.⁷⁴ A penetration of ionic sodium into chromium oxide occupying similar sites as in these compounds is therefore conceivable.

The corresponding decay spectra of the $KL_{23}L_{23}$ Auger type also reveal chemical shifts, and may be interpreted accordingly. Fig. 11(a) and 11(b) show the data taken for a deposition experiment and for a desorption experiment, respectively. Three chemically different species can be identified giving rise to Auger features at 989.5, 991.5 and 994.8 eV. The feature at the highest kinetic energy and high coverage is easiest to identify, because it is accompanied by intense plasmon losses typical for surface and bulk plasmons of metallic sodium layers.⁷⁵ There are two species present at low sodium coverage (B, C). That at the lower kinetic energy dominates at the lowest coverages (B), while the one with higher kinetic energy dominates at somewhat higher coverages (C), *i.e.*, near the maximum workfunction change around the minimum. Around monolayer coverage (D) the spectral features shift towards the metallic situation.

An attempt to assign the degree of ionicity of the species can be made on the basis of a so-called Wagner plot⁷⁶⁻⁷⁸ (see Fig. 12), where the Na 1s binding energies are plotted *vs.* the Auger kinetic energies. The Auger parameter, which is characteristic for the final state relaxation in the system, can be used to classify the ionicity of the species.⁷⁹

The disappearance of the species giving rise to the photoemission feature at 31.5 eV Na 2p binding energy (Fig. 10) is paralleled by the appearance of a signal in the sodium $KL_{23}L_{23}$ Auger at 988 eV (Fig. 11). This indicates the existence of an ionic, fully coordinated sodium species as also supported by a comparison with ionic sodium compounds in literature.⁸⁰ Furthermore, we ascribe the Auger line at 991.5 eV to the adsorbed neutral sodium atoms. The calculation of the expected kinetic energy in this case is much more complicated than it was for the photoemission binding energy; as the initial and the final state of the Auger transition are ionic species they will couple much more strongly to the substrate than the neutral species does in the ground state. Hence, the proper reference level is the Fermi level rather than the vacuum level. With these considerations in mind we can now understand qualitatively the chemical shift of the sodium atoms relative to the ionic species if, in addition, we consider the chemical shifts of the Auger spectra of sodium halides.⁸⁰ The shifts are small and even change sign

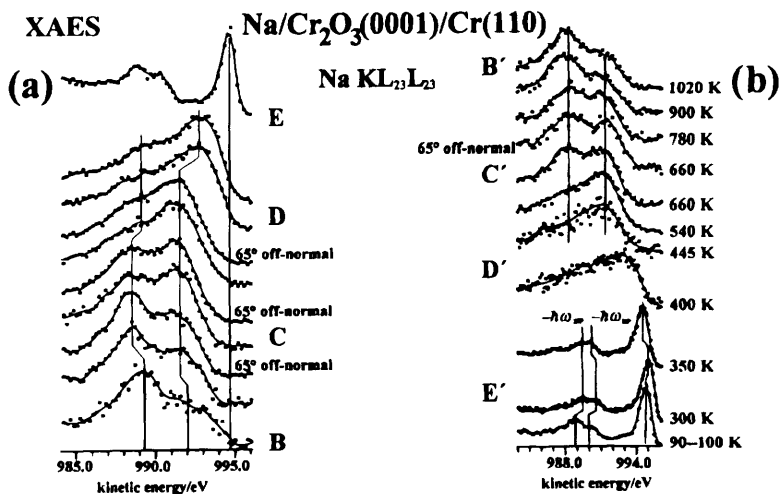


Fig. 11 Na $KL_{23}L_{23}$ X-ray Auger emission (XAE) spectra in: (a) a sodium deposition experiment on $Cr_2O_3(0001)/Cr(110)$ induced at 90 K; and (b) a heating experiment on multilayers of sodium on $Cr_2O_3(0001)/Cr(110)$. If not otherwise stated the spectra were taken at 15° off-normal detection angle.

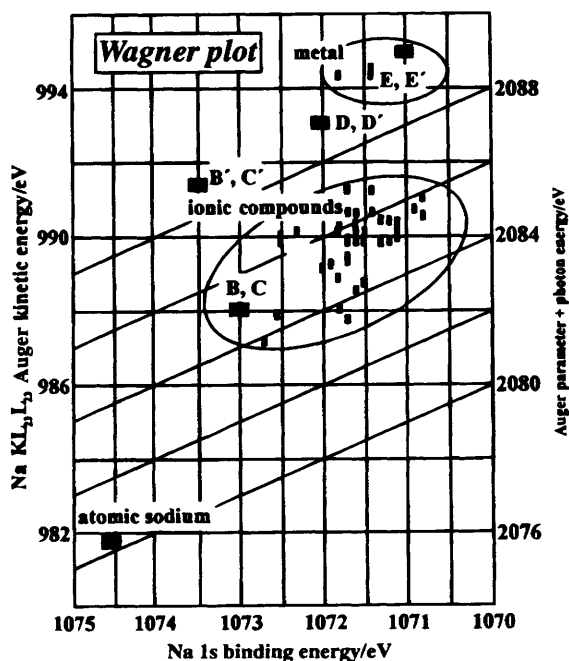


Fig. 12 Wagner plot adapted from ref. 77. The binding and Auger energy of atomic sodium were taken from ref. 78 and referenced to the Fermi level by subtraction of the workfunction of sodium metal.

going from NaF to NaI. However, Auger electrons from sodium metal are abnormally shifted to higher kinetic energies due to its metallic state. For neutral but non-metallic sodium species this abnormally large shift does not exist. Thus it becomes plausible that the Auger line position of sodium atoms are found in the same regime in the Wagner plot as compared with the ionic species.

The KLL Auger spectra also provide clear evidence for the diffusion of sodium into the chromium oxide film by comparison with the Na 2p photoemission data. Although the Auger electrons carry a kinetic energy of close to 1 keV and thus reach an escape depth of 10–15 Å, the Na 2p photoelectrons have a kinetic energy of 120 eV and therefore only escape from the topmost layers.⁸¹ Hence, whereas the photoemission data indicate loss of sodium from the sample surface, the Auger data reveal its diffusion into deeper layers of the sample. Also TDS reveals desorption into the gas phase; data starting from different initial coverages are shown in Fig. 13. In the submonolayer coverage regime, the desorption peak shifts as a function of coverage from a temperature of 750 to 500 K. After completion of the first monolayer, a second feature with smaller linewidth grows at a peak temperature of 400 K, which is identical for the onset of multilayer desorption (as revealed in the workfunction data and electron emission data). As discussed above, the only sodium species present on the surface at temperatures as high as 600–1000 K is atomic sodium. We can conclude that this atomic, non-ionic species serves as a precursor for thermal desorption in the experiment in Fig. 13.

At this point it is appropriate to investigate the response of the oxide substrate towards the adsorption of sodium. Fig. 14(a) and (b) show Cr 2p_{3/2} photoemission data in a desorption experiment as a function of temperature for both near-normal and grazing exit detection, respectively. The clean chromium oxide surface leads to a typical lineshape of the Cr 2p_{3/2} spectra. This lineshape is characteristic of coordinately unsatu-

TDS Na/Cr₂O₃(0001)/Cr(110)

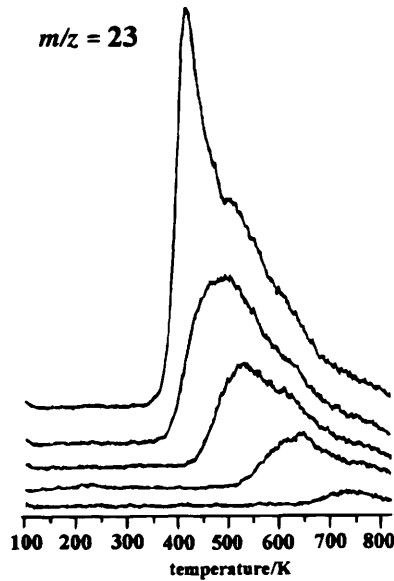


Fig. 13 TD spectra of the system Na/Cr₂O₃(0001)/Cr(110) detecting sodium monomers in the channel $m/z = 23$. The spectra are ascending with increasing coverage.

rated Cr³⁺ ions on the surface and coordinately saturated Cr³⁺ ions in the bulk. Upon adsorption of sodium this lineshape changes, but there is no indication for the formation of metallic chromium. We show for comparison the spectrum of the metallic chromium substrate on the correct energy scale, and recall the corresponding data for magnesium

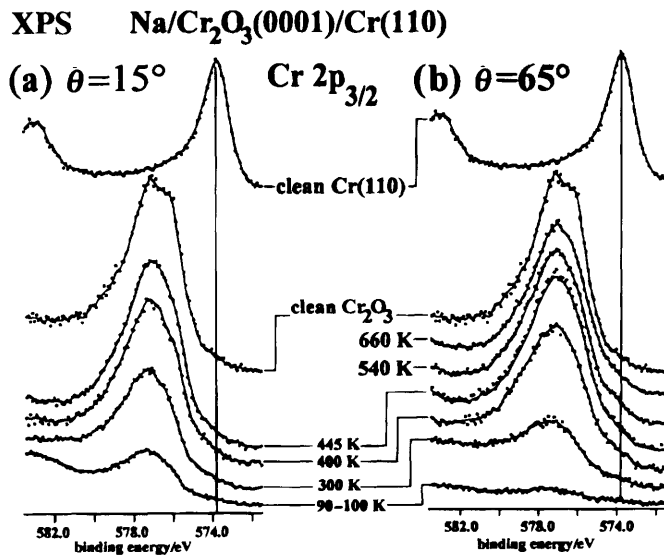


Fig. 14 Cr 2p_{3/2} XP spectra of the system Na/Cr₂O₃(0001)/Cr(110) taken in a heating experiment with an initial multilayer sodium coverage. (a) Taken at near-normal detection angle; and (b) taken at grazing detection angle.

deposition where the formation of metallic chromium in the equivalent experiment has been clearly observed.⁴⁸ We confirm that at lower coverages sodium forms non-metallic surface species without reducing the surface chromium ions in the oxide to the metallic state.

Finally, the following discussion of the EEL spectra can be taken to determine the oxidation state of the chromium ions in the surface after sodium deposition. Fig. 15 shows EEL spectra of a heating experiment. Here the oxide surface has been initially dosed at 90 K with a thick sodium layer. The surface is heated to the temperature given, and subsequently cooled to liquid-nitrogen temperature, where the spectra are then recorded again. Clearly, compared with the clean oxide surface the spectrum of the surface covered with a thick sodium overlayer is rather structureless, except for features at excitation energies of 4 eV and 0.8 eV. Both features can be assigned to the excitation of surface and interface plasmons.⁸² The relatively wide feature at an excitation energy of 4 eV can be easily assigned to a surface plasmon excitation of the thick sodium film. The surface plasmon energy scales with $\sqrt{2}$ of the bulk plasmon energy,^{71,75} which is found near an excitation energy of 6 eV. We attribute the second feature to the excitation of a plasmon localized at the interface of the sodium film and the thick chromium oxide layer. The two plasmons therefore represent the two interface solutions of a metallic layer sandwiched between a vacuum on one side and a dielectric on the other side. Such systems have been discussed in the literature, and it is well known⁸² that the frequencies of the interface plasmons depend on the thickness of the metallic layer. The vacuum/metal interface plasmon frequency is expected to depend more strongly on the thickness of the metal layer than the metal/dielectric interface plasmon frequency,⁸² the latter being basically pinned at a given energy. This behaviour is observed experimentally. The surface plasmon frequency shifts to smaller values, *i.e.*, from 4 to 2.9 eV, upon

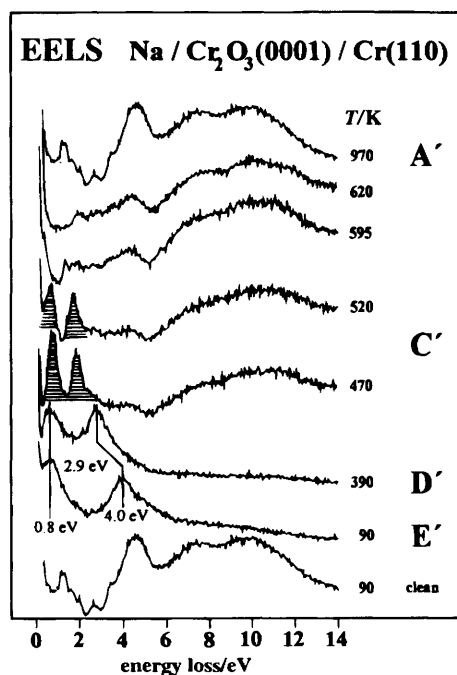


Fig. 15 EEL spectra of the system Na/Cr₂O₃(0001)/Cr(110) taken in a heating experiment with an initial multilayer sodium coverage. The system was heated to the temperature given, cooled back to 90 K and then the spectra were recorded.

partial desorption of sodium from the surface by increasing the surface temperature from 90 to 390 K. Above 450 K the sodium coverage reaches monolayer coverage, and correspondingly the electronic excitation spectrum changes considerably. First, upon raising the temperature there is no longer a continuous shift of excitation energies, indicating the localized nature of the excitations. Secondly, the linewidths of the spectral features decrease considerably, which is also indicative of the local nature of the excitation process. Near 600 K, where most of the sodium has been removed from the surface, the electronic excitations characteristic for the undistorted chromium oxide surface start to reappear. Close to 1000 K the surface excitations of the clean Cr_2O_3 surface have completely reappeared.

In order to assign the electronic excitations for the monolayer coverage, Volker Staemmler and his group have performed cluster calculations⁸³ very similar to those performed earlier for Cr^{3+} ions localized in the various possible sites at an ideal $\text{Cr}_2\text{O}_3(0001)$ surface. The most prominent results of the calculation is that there are two low lying states, one near 0.8 eV and another one near 2.0 eV, in close agreement with the most prominent features in the EEL spectra. Of course, there are excitations above 2 eV predicted in the calculation that do not show intense counterparts in the experimental spectra. However, the prediction of intensities in EEL spectra is a rather difficult task, and cannot be performed routinely at present. Therefore a definite assignment based on calculated excitation energies and intensities cannot be given at this time. It is a general observation⁷ that the intensities of the d-d excitations within the oxide band-gap decrease as the excitation energy approaches the band-gap energy where strong mixing with oxygen-metal charge transfer excitations comes into play. Summarizing the results of the theoretical predictions we take the close agreement of the calculated and experimentally observed excitation energies as a strong indication that the Cr ions in the oxide surface, in the presence of a submonolayer sodium coverage, change and are possibly in oxidation state 2+ in line with chemical intuition.

Coadsorption of ethene and sodium

At this point it is interesting to investigate the influence of sodium on the oxide surface on adsorption of other molecules. Fig. 16 shows a series of RAIR spectra taken after dosing an Na-precovered $\text{Cr}_2\text{O}_3(0001)$ surface with 10 L ethene. In the first experiment [Fig. 16(a)] various amounts of sodium were evaporated onto the surface at 90 K. In the second experiment [Fig. 16(b)], a surface covered with a submonolayer of sodium was subsequently heated to higher temperatures. After this procedure, ethene was admitted at 90 K.

The regions of the C—H stretch and the C—H wagging modes are shown. The lowest trace in Fig. 16(a) is equivalent to the spectrum shown in Fig. 7. Both vibrations are observed and are, as discussed above, due to the presence of a weakly π -bonded ethene (no C—H stretch) and a physisorbed species (both C—H stretch and C—H wagging mode). On the sodium precovered surface, ethene is adsorbed as long as there are sites available on the oxide surface. For higher Na coverages ethene is not adsorbed, as documented by the spectrum at the top of Fig. 16(a). At intermediate coverage the C—H stretching vibration is observed with rather high intensity but its frequency is slightly red-shifted with respect to the clean surface.

However, more interestingly, no C—H wagging vibration is observed at sodium precoverage. In addition, if the sodium precoverage is near the coverage characteristic for the workfunction minimum the C—H stretching vibrational band is split [Fig. 16(b)]. A more detailed temperature dependent analysis reveals that this splitting is due to the presence of two different chemical species on the surface, this is in turn compatible with the presence of two different sodium species, as identified with photoemission and Auger spectroscopy (see above).

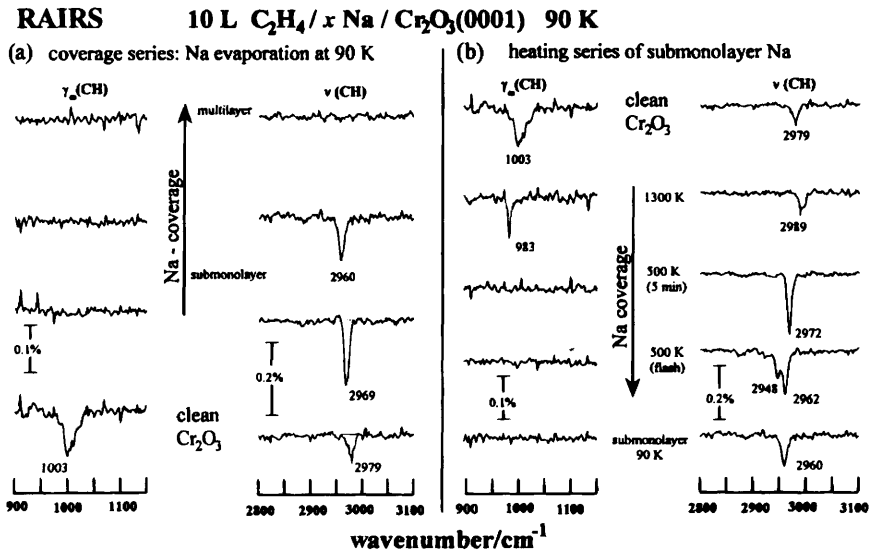


Fig. 16 RAIR spectra of adsorption of C₂H₄ on Na/Cr₂O₃(0001)/Cr(110) at 90 K. The sodium coverages were prepared by: (a) deposition of small amounts of sodium at 90 K; and (b) heating of an initial submonolayer coverage of sodium.

Obviously Na influences the adsorption properties of ethene. TD spectra (not shown), however, indicate a small change in desorption energy only. Comparison with corresponding RAIRS studies of ethene adsorption on metal surfaces provides us with a hint towards an interpretation of the data. Briefly, on metal surfaces there have been π -bonded as well as di- σ -bonded ethene adsorbates identified.⁸⁴ For example, on a clean Pt(111) surface ethene is thought to be adsorbed as a di- σ -complex.⁸⁵ In this bonding mode the CH-wagging mode is extremely weak. If oxygen is co-adsorbed onto the Pt(111) surface, ethene is believed to be π -bonded with an internal CH-wagging mode in the vibrational spectrum.^{86,87} Parallel to this we interpret the finding at the oxide surface as the conversion of π -bonded ethene on the clean surface to a di- σ -bonded complex on the sodium precovered oxide surface. Further experiments confirm this preliminary interpretation and it is quite conceivable that the electron-rich chromium ions allow for the formation of the two σ -bonds with the ethene moiety, while the more electron deficient, clean oxide surface only stabilizes a π -donor interaction from ethene towards the surface.

These findings will have to be explored with respect to the influence of the reactivity of the modified ethene towards other species co-adsorbed onto the surface.

Conclusions

We have investigated adsorption and reaction of molecules on a structurally well characterized polar oxide surface, *i.e.*, the Cr₂O₃(0001) surface. Oxygen is adsorbed molecularly below room temperature *via* formation of a moderately strong chemisorptive bond. It is partly desorbed molecularly at room temperature and another fraction dissociates on the surface under formation of chromyl species (*i.e.*, Cr=O double bonds) on the surface. Although the molecular species does not exchange with the lattice oxygen, there is some exchange of the atomic species.

Oxygen chemisorption very strongly influences adsorption of other molecules, such as ethene. While ethene is chemisorbed on the clean surface with planar orientation as a

π -complex on the chromium ions, pre-adsorption of oxygen attenuates the ethene surface coverage, allowing it only to be adsorbed on those sites not oxygen covered (*i.e.*, defects). The intermolecular interaction is not negligible but rather moderate. Consequences of site blocking by oxygen are, however, not negligible as indicated by the considerable reduction in the ethene polymerization activity of the surface.

Other adsorbates, such as Na, have a pronounced influence on adsorption of other molecules, because they induce charge transfer to the surface. Na grows on the $\text{Cr}_2\text{O}_3(0001)$ surface in a Frank van der Merwe mode, similar to the situation found for Na adsorption on a metal surface. In the submonolayer regime sodium ions and concomitantly probably Cr^{2+} ions as well as neutral sodium atoms are formed. While sodium ions migrate into the oxide at elevated temperature, sodium atoms are desorbed from the surface into the gas phase. If ethene is co-adsorbed it seems to change its bonding characteristics as compared with the Na free surface. The RAIR spectra are compatible with the formation of a di- σ -bonded species in contrast to a π -bonded complex on the clean surface. Whether this finding has consequences for the reactivity of ethene towards other co-adsorbed molecules remains to be seen.

We are grateful to the agencies that have supported our work: Deutsche Forschungsgemeinschaft, Bundesminister für Bildung und Forschung, Ministerium für Wissenschaft und Forschung des Landes Nordrhein-Westfalen and Fonds der Chemischen Industrie. G.K. and I.N.Y. received a fellowship from the Graduiertenkolleg 'Dynamische Prozesse an Festkörperoberflächen'. O.S. is grateful for the receipt of a stipendium from the Studienstiftung des Deutschen Volkes.

References

- 1 C. Noguera, *Physics and Chemistry at Oxide Surfaces*, Cambridge University Press, Cambridge, 1996.
- 2 V. E. Henrich and P. A. Cox, *The Surface Science of Metal Oxides*, Cambridge University Press, Cambridge, 1994.
- 3 *Adsorption on Ordered Surfaces of Ionic Solids and Thin Films*, ed. H-J. Freund and E. Umbach, Springer Series in Surface Sciences, vol. 33, Springer Verlag, Heidelberg, 1993.
- 4 C. Xu and D. W. Goodman, in *Handbook of Heterogeneous Catalysis*, ed. G. Ertl, H. Knözinger and J. Wertkamp, Verlag Chemie, Weinheim, ch. 4.6, in press.
- 5 H-J. Freund, *Ber. Bunsen-Ges. Phys. Chem.*, 1995, **99**, 1261.
- 6 H-J. Freund, H. Kuhlbeck and V. Staemmler, *Rep. Prog. Phys.*, 1996, **59**, 283.
- 7 H-J. Freund, *Phys. Status Solidi B*, 1995, **192**, 407.
- 8 H-J. Freund, NATO ASI Series C, Kluwer Academic, 1996, vol. 474, p. 232.
- 9 H. Kuhlbeck, *Appl. Phys. A*, 1994, **59**, 469.
- 10 (a) N. G. Condon, P. W. Murray, F. M. Leibsle, G. Thornton, A. R. Lennie and D. J. Vaughan, *Surf. Sci.*, 1994, **310**, 2609; (b) A. R. Lennie, N. G. Condon, F. M. Leibsle, P. W. Murray, G. Thornton and D. J. Vaughan, *Phys. Rev. B*, 1996, **53**, 10244; (c) J-W. He and P. J. Møller, *Chem. Phys. Lett.*, 1986, **129**, 13; (d) P. J. Møller, in *Science of Ceramic Interfaces II*, ed. J. Nowotny, 1994, p. 473.
- 11 T. E. Madey, U. Diebold and J-M. Pan, in *Adsorption on Ordered Surfaces of Ionic Solids and Thin Films*, Springer Series in Surface Science, ed. H-J. Freund and E. Umbach, Springer Verlag, Heidelberg, 1993, vol. 33, p. 147.
- 12 (a) W. Weiss, A. Barbieri, M. A. van Hove and G. A. Somorjai, *Phys. Rev. Lett.*, 1993, **71**, L1848; (b) A. Barbieri, W. Weiss, M. A. van Hove and G. A. Somorjai, *Surf. Sci.*, 1994, **302**, 259.
- 13 D. Schmalzried, *Chemical Kinetics of Solids*, Verlag Chemie, Weinheim, 1995.
- 14 *Catalyst Supports and Supported Catalysts*, ed. A. B. Stiles, Butterworth, Boston, 1987.
- 15 *Metal Clusters in Catalysis*, ed. B. C. Gates, L. Gucci and H. Knözinger, Studies in Surface Science and Catalysis, Elsevier, Amsterdam, vol. 29, 1986.
- 16 H. Kuhlbeck, G. Odörfer, R. M. Jäger, G. Illing, M. Menges, Th. Mull, H-J. Freund, M. Pöhlchen, V. Staemmler, S. Witzel, C. Scharfschwerdt, K. Wennemann, T. Liedtke and M. Neumann, *Phys. Rev. B*, 1991, **43**, 1969.
- 17 M. Haßel and H-J. Freund, *Surf. Sci.*, 1995, **325**, 163.
- 18 D. Cappus, M. Haßel, E. Neuhaus, M. Heber, F. Rohr and H-J. Freund, *Surf. Sci.*, 1995, **337**, 268.
- 19 P. W. Tasker, *J. Phys. C: Solid State Phys.*, 1979, **12**, 4977.
- 20 P. W. Tasker, *Philos Mag. A*, 1979, **39**, 119.

- 21 R. Lacmann, *Colloq. Int. C.N.R.S.*, 1965, **152**, 195.
- 22 D. Wolf, *Phys. Rev. Lett.*, 1992, **68**, L3315.
- 23 A. Freitag, Dissertation, Ruhr-Universität Bochum, 1995.
- 24 D. Cappus, C. Xu, D. Ehrlich, B. Dillmann, C. A. Ventrice Jr., K. Al-Shamery, H. Kuhlenbeck and H-J. Freund, *Chem. Phys.*, 1993, **177**, 533.
- 25 K. Refson, R. A. Wagelies, D. G. Fraser, M. C. Payne, M. H. Lee and V. Milan, *Phys. Rev. B*, 1995, **52**, 10833.
- 26 C. G. Kinniburgh, *J. Phys. C: Solid State Phys.*, 1975, **8**, 2382.
- 27 M. R. Welton-Cook and W. Berndt, *J. Phys. C: Solid State Phys.*, 1982, **15**, 5691.
- 28 T. Urano, T. Kanaji and M. Kaburagi, *Surf. Sci.*, 1983, **134**, 109.
- 29 D. L. Blanchard, D. L. Lessor, J. P. LaFemina, D. R. Baer, W. K. Ford and T. Guo, *J. Vac. Sci. Technol. A*, 1991, **9**, 1814.
- 30 C. G. Kinniburgh and J. A. Walker, *Surf. Sci.*, 1977, **63**, 274.
- 31 R. C. Felton, M. Prutton, S. P. Tear and M. R. Welton-Cook, *Surf. Sci.*, 1979, **88**, 474.
- 32 K. H. Rieder, *Surf. Sci.*, 1982, **148**, 37.
- 33 R. Gerlach, A. Glebov, G. Lange, J. P. Toennies and H. Weiss, *Surf. Sci.*, 1995, **331-333**, 2490.
- 34 (a) S. M. Vesecky, C. Xu and D. W. Goodman, *J. Vac. Sci. Technol. A*, 1994, **12**, 2114; (b) M. C. Wu, C. M. Truong and D. W. Goodman, *J. Phys. Chem.*, 1993, **97**, 4182; (c) C. M. Truong, M. C. Wu and D. W. Goodman, *J. Am. Chem. Soc.*, 1993, **115**, 3647; (d) J. W. He, J. S. Corneille, C. A. Estrada, M. C. Wu and D. W. Goodman, *J. Vac. Sci. Technol. A*, 1992, **10**, 2248; (e) M. C. Wu, C. A. Estrada, J. S. Corneille and D. W. Goodman, *J. Chem. Phys.*, 1992, **96**, 3892.
- 35 J. Heidberg and D. Meine, *Ber. Bunsen-Ges. Phys. Chem.*, 1993, **97**, 211.
- 36 A. Zecchina, D. Scarano, S. Bordiga, G. Ricchiardi, G. Spoto and F. Geobaldo, *Catal. Today*, 1996, **27**, 403.
- 37 D. Cappus, J. Klinkmann, H. Kuhlenbeck and H-J. Freund, *Surf. Sci. Lett.*, 1995, **325**, L421.
- 38 G. Pacchioni and P. S. Bagus, in *Adsorption on Ordered Surfaces of Ionic Solids and Thin Films*, ed. H-J. Freund and E. Umbach, Springer Series in Surface Science, Springer Verlag, Heidelberg, 1993, vol. 33, p. 180.
- 39 F. Rohr, K. Wirth, J. Libuda, D. Cappus, M. Bäumer and H-J. Freund, *Surf. Sci. Lett.*, 1994, **315**, L2977.
- 40 H. Kuhlenbeck, C. Xu, B. Dillmann, M. Häbel, B. Adam, D. Ehrlich, S. Wohlrab, H-J. Freund, U. A. Ditzinger, H. Neddermeyer, M. Neuber and M. Neumann, *Ber. Bunsen-Ges. Phys. Chem.*, 1992, **96**, 15.
- 41 C. A. Ventrice Jr., D. Ehrlich, E. L. Garfunkel, B. Dillmann, D. Heskett and H-J. Freund, *Phys. Rev. B*, 1992, **46**, 12892.
- 42 M. Bender, D. Ehrlich, I. N. Yakovkin, F. Rohr, M. Bäumer, H. Kuhlenbeck, H-J. Freund and V. Staemmler, *J. Phys.: Condens. Matter*, 1995, **7**, 5289.
- 43 C. Xu, M. Häbel, H. Kuhlenbeck and H-J. Freund, *Surf. Sci.*, **258**, 23.
- 44 C. Xu, B. Dillmann, H. Kuhlenbeck and H-J. Freund, *Phys. Rev. Lett.*, 1991, **67**, 3551.
- 45 F. Rohr, M. Bäumer, H-J. Freund, S. Müller, L. Hammer and K. Heinz, *Surf. Sci.*, in press.
- 46 M. Causa and C. Pisani, *Surf. Sci.*, 1989, **215**, 271.
- 47 F. Manassidin, A. Devita and M. Gillan, *Surf. Sci. Lett.*, 1993, **285**, L517.
- 48 M. Bender, I. N. Yakovkin and H-J. Freund, *Surf. Sci.*, 1996, **365**, 394.
- 49 J. J. Yeh and I. Lindau, *At. Data Nucl. Data Tables*, 1985, **32**, 2.
- 50 K. P. Huber and G. Herzberg, *Molecular Spectra and Molecular Structure, IV: Constants of Diatomic Molecules*, Van Nostrand Reinhold, New York, 1979.
- 51 H-J. Freund, B. Dillmann, O. Seiferth, G. Klivenyi, M. Bender, D. Ehrlich, I. Hemmerich and D. Cappus, *Catal. Today*, in press.
- 52 (a) A. Bakac, S. L. Scott, J. H. Espenson and K. R. Rodgers, *J. Am. Chem. Soc.*, 1995, **117**, 6483; (b) J. Rolfé, *J. Chem. Phys.*, 1968, **49**, 963.
- 53 (a) N. D. S. Canning and M. A. Chesters, *J. Electron Spectrosc. Relat. Phenom.*, 1983, **30**, 247; (b) J. L. Gland, B. A. Sexton and G. B. Fisher, *Surf. Sci.*, 1980, **95**, 587; (c) K. Prabhakaran and C. N. R. Rao, *Surf. Sci.*, 1987, **186**, L575.
- 54 (a) F. A. Miller, G. L. Carlton and W. B. White, *Spectrochim. Acta*, 1959, **15**, 709; (b) W. E. Hobbs, *J. Chem. Phys.*, 1958, **28**, 1220.
- 55 B. Dillmann, Dissertation, Ruhr-Universität Bochum, 1996.
- 56 F. Rohr, Dissertation, Ruhr-Universität Bochum, 1996.
- 57 J. H. Lunsford, X. Yang, K. Haller, J. Laane, G. Mestl and H. Knözinger, *J. Phys. Chem.*, 1993, **97**, 13810.
- 58 M. Häbel, Diploma Thesis, Ruhr-Universität Bochum, 1991.
- 59 R. M. Jaeger, J. Libuda, M. Bäumer, K. Homann, H. Kuhlenbeck and H-J. Freund, *J. Electron Spectrosc. Relat. Phenom.*, 1993, **64/65**, 217.
- 60 (a) P. J. M. Carrott and N. Sheppard, *J. Chem. Soc., Faraday Trans. I*, 1983, **79**, 2425; (b) A. A. Davydov, Y. M. Shechekochikhin and N. P. Keier, *Kinet. Katal.*, 1972, **13**, 1088; (c) I. E. Wachs, *Catal. Today*, in press; (d) A. Zecchina, S. Coluccia, L. Cerruti, E. Borella, *J. Phys. Chem.*, 1971, **75**, 2783.

- 61 M. Pinzolit, W. Hebenstreit, M. Schmid and P. Varga, *Untersuchungen der Segregation von Verunreinigungen an Cr(100) mittels STM-Messungen*, DPG Frühjahrstagung 1996, Regensburg, Abstract (O 25.4).
- 62 I. Hemmerich, F. Rohr, O. Seiferth, B. Dillmann and H-J. Freund, *Z. Phys. Chem. NF*, in press.
- 63 H. Ibach and D. L. Mills, *Electron Energy Loss Spectroscopy and Surface Vibrations*, Academic Press, New York, 1982.
- 64 M. P. McDaniel, *Adv. Catal.*, 1985, **33**, 47.
- 65 (a) D. D. Beck and J. H. Lunsford, *J. Catal.*, 1981, **68**, 121; (b) D. L. Myers and J. H. Lunsford, *J. Catal.*, 1986, **92**, 260; (c) D. L. Myers and J. H. Lunsford, *J. Catal.*, 1986, **99**, 140.
- 66 J. S. Foord and R. M. Lambert, *Surf. Sci.*, 1986, **169**, 327.
- 67 M. Bender, K. Al-Shamery and H-J. Freund, *Langmuir*, 1994, **10**, 3081.
- 68 D. Heskett, D. Tang, X. Shi, C. Su and K-D. Tsuei, *J. Phys.: Condens. Matter*, 1994, **6**, 13.
- 69 H. Ishida and A. Liebsch, *Phys. Rev. B*, 1990, **42**, 5505 and references cited therein.
- 70 *Handbook of Physics and Chemistry*, 53rd edn. CRC Press, Cleveland, OH, 1972.
- 71 A. Barrie and F. J. Street, *J. Electron Spectrosc. Relat. Phenom.*, 1975, **7**, 1.
- 72 P. H. Citrin and T. D. Thomas, *J. Chem. Phys.*, 1972, **57**, 4446.
- 73 S. Krummacher, V. Schmidt, J. M. Bizau, D. L. Ederer, P. Dhez and F. Wuilleumier, *J. Phys. B: At. Mol. Phys.*, 1982, **15**, 4363.
- 74 H. Kadowaki, H. Takei and K. Motoya, *J. Phys.: Condens. Matter*, 1995, **7**, 6869 and references cited therein.
- 75 J. C. Fuggle in *Electron Spectroscopy: Theory, Techniques and Applications*, ed. C. R. Brundle and A. D. Baker, Academic Press, London, 1981, vol. 4, p. 85.
- 76 (a) C. D. Wagner, *Faraday Discuss. Chem. Soc.*, 1975, **60**, 291; (b) C. D. Wagner, *J. Electron Spectrosc. Relat. Phenom.*, 1977, **10**, 305.
- 77 C. D. Wagner, in *Handbook of Photoelectron Spectroscopy*, ed. J. F. Moulder, W. F. Stickle, P. E. Sobol and K. D. Bomber, Perkin-Elmer Corp., Eden Prairie, MN, 1992.
- 78 R. L. Martin, E. R. Davidson, M. S. Banna, B. Wallbank, D. C. Frost and C. A. McDowell, *J. Chem. Phys.*, 1978, **68**, 5006.
- 79 G. Hohlneicher, H. Pulm and H-J. Freund, *J. Electron Spectrosc. Relat. Phenom.*, 1985, **37**, 209.
- 80 V. I. Nefedov, V. G. Yarzhemsky, A. V. Chuvaev, E. M. Trishkina, *J. Electron Spectrosc. Relat. Phenom.*, 1988, **46**, 381.
- 81 M. P. Seah, W. A. Dench, *SIA Surf. Interf. Anal.*, 1979, **1**, 2.
- 82 H. Raether, *Solid State Excitations by Electrons*, in Springer Tracts in Modern Physics, Springer, New York, 1965, vol. 38.
- 83 V. Staemmler, personal communication.
- 84 N. Sheppard, *Annu. Rev. Phys. Chem.*, 1988, **39**, 589.
- 85 J. Fan and M. Trenary, *Langmuir*, 1994, **10**, 3649; J. Kubota, S. Ichihara, J. N. Kondo, K. Domen and C. Hirose, *Langmuir*, 1996, **12**, 1926.
- 86 H. Steininger, H. Ibach and S. Lehwald, *Surf. Sci.*, 1982, **117**, 685.
- 87 R. L. Martin, E. R. Davidson, M. S. Banna, B. Wallbank, D. C. Frost and C. A. McDowell, *J. Chem. Phys.*, 1978, **68**, 5006.